International Journal of Safety and Security Engineering
Vol. 15, No. 1, January, 2025, pp. 127-139
Journal homepage: http://iieta.org/journals/ijsse

Expansive Residual Soil Stability Behavior During Wetting and Drying Process

Putera Agung Maha Agung[1*], Sony Pramusandi[1], Andikanoza Pradiptiya[1], Aldo Wirastana Adinegara[1], Suripto[1], Muhammad Idris[2], Ramlan Sultan[2], Muhammad Fathur Rouf Hasan[3], Adnan Zainorabidin[4]

[1] Department of Civil Engineering, Politeknik Negeri Jakarta, Depok 16425, Indonesia
[2] Department of Civil Engineering, Politeknik Negeri Ujung Pandang, Makassar 90245, Indonesia
[3] Department of Environmental Science, Postgraduate School, Universitas Brawijaya, Malang 65145, Indonesia
[4] Faculty of Civil Engineering and Built Environment, University Tun Hussein Onn Malaysia, Johor 86400, Malaysia

Corresponding Author Email: putera.agungmagung@sipil.pnj.ac.id

https://doi.org/10.18280/ijsse.150114

Received: 3 November 2024
Revised: 26 December 2024
Accepted: 12 January 2025
Available online: 31 January 2025

Keywords:
deformation, expansive residual soil, coefficient of permeability, SWCC, stability analysis, unsaturated

ABSTRACT

Indonesia's climate change, with extreme temperature and rainfall intensity fluctuations, can trigger slope sliding. The water infiltration process on unsaturated expansive residual soil types can significantly fail at the slope zone due to increasing pore water pressure in the short term. A high swelling and shrinkage due to changes in water content can generate initial movement to the toe of the slope. This study aims to select a research method to define the magnitude of deformation and safety factor (SF) of stability conditions, considering the best fit for the soil water characteristic curve (SWCC). The preparation of soil parameters during simulation is supported by physical and mechanical properties at the soil mechanic laboratory. The results indicated that the dry season was more stable than the rainy or wet season. Deformation during dry conditions (dry season) was smaller than 1.0 inch (25,4 mm) with the safety value (SF) of slope sliding larger than 1.20 and vice versa, during wet conditions (rainy season) would occur (SF = 0.152).

1. INTRODUCTION

Generally, Indonesia is one of the largest archipelago countries in Southeast Asia, geographically crossed by the equator, and has a major tropical climate. The rainy and dry seasons are significant factors in the formation of a soil deposit to be unsaturated. Therefore, unsaturated fine-grained soils with negative pore-water pressures can fundamentally form on geological residual deposits due to the weathering process of granite and / or sedimentary rocks, such as residual layer soil. This type of layer is often found in West Java River watersheds and / or basin areas, such as the Cisadane River located in the South Tangerang District.

Residual formation areas found in watersheds, river basins, river estuaries, seas, etc., can be classified as expansive or non-expansive soils, which is dependent on the plasticity index (PI) value. Residual soils can cover 80% - 90% of the mainland especially. There is not much has been performed to handle cases resulting from problems caused by especially expansive residual soils, if there is an attempt or effort, it will be carried out with poor handling for soil improvement.

As a fine-grained soil deposit, the unsaturated expansive residual soil near the ground surface of the slope failure has two important problems due to rainfall infiltration, such as increasing pore-water pressure and swelling-shrinkage potential caused by the content of montmorillonite [1, 2]. Both problems can reduce the soil shear strength during the wetting-drying process. Characteristics of the slope failure on residual soil as unsaturated soil are its heterogeneity, a grain size distribution with relatively diverse variations and unlimited conditions [3, 4]. Many studies or references exist on slope failure of unsaturated expansive residual soil.

Many researchers have studied relating to rainfall and reducing matric suction in the shallower soil layers. Sorbino and Nicotera [5] investigated rainfall-induced flow landslides in coarse-grained soils. Kim et al. [6] described a physical-based model to predict rainfall-induced landsides using GIS-based and YS-Slope models and Darcy's law model to evaluate the susceptibility of landslides. Gui and Wu [7] found that infiltration of water reduced the matric suction of the soil by the generation of excess pore-water pressure, and a reduction in shear strength did not accompany it. Unsaturated soil failed under a constant shear stress applied prior to the infiltration. Excessive deformation and the eventual softening of the soil were found to be the main causes of water infiltration induced failure.

On average of their opinions, almost of their studies used the matric suction database without consideration a significant change occurs when the soil is imposed by a low-high suction range, specifically for shallower soil layers [8]. Furthermore, focus attention is only on a shear strength without calculating the high matric suction due to the wetting-drying at the layers near the ground surface in evaluating landslide potential [9].

Most slope failure is dominated by saturated residual soil type during the rainy season due to the enhancement condition of increasing pore water pressure. However, understanding the behavior of saturated soil is not enough to evaluate landslide potential, especially from the ground surface to the depth of -

5.00 m. At these depths, unsaturated soil analysis would be necessary to describe the soil behavior accurately in the field; most of the soil behavior can be influenced by matric suction, especially when soil shear strength is determined when the transformation of water content occurs.

When the water content changes, positive or negative pore water pressure may have occurred during the alternation of weather, dry or rainy season. A soil layer with a depth of less than -5.00 m, called an unsaturated zone (vadose zone), will have a low-high suction and be most influenced by the boundary condition of flux water due to the evaporation and infiltration process [10]. In an indirect condition, soil suction has an important role in increasing or decreasing soil shear strength, especially in vadose zones. On several issues in geotechnical engineering, specifically expansive residual soil, it has a high swelling and shrinkage potential due to the alteration of volumetric water content for shallow landslides [11]. When infrastructure construction, the magnitude of volumetric water content and volume change on expansive residual soil could reduce the soil shear strength and generate some cracks at the ground surface; finally, it will create a landslide gradually or a differential settlement that destroys the upper structure [12]. However, it is very difficult to determine the transformation of volumetric water content in the transition phase or between saturated and unsaturated phases when applying the soil water characteristic curve (SWCC) based on the water permeability function. Modelling at laboratory works and mathematical analysis is insufficient to determine the air-entry value, inflection point, and residual point that will define the true residual water content and be matched to the behavior in the field. The selection of the SWCC best-fil curve and permeability function is important in measuring the reduction and increase of strength parameters for cohesion (c) and internal friction angle (ϕ) during the wetting and drying process.

This study aims to define problem solving practically using the best fit of soil water characteristic curve (SWCC) and permeability function depending on suction condition as the input data for simulation stability analysis. The measurement of soil suction uses the filter paper method to determine SWCC and permeability function. The selection parameter process of SWCC and permeability function are performed by the theory of probabilistic analysis using several references [13, 14]. Trial-and-error procedures under wetting-drying are applied to define the best-fit of SWCC and water permeability function, then all the parameter results will be investigated again at the laboratory works for validation of coefficient of permeability and shear strength parameters *(c; ϕ)* under wetting-drying conditions. These validated parameters will be used as input data in the prediction of the magnitude of soil deformation (axial and lateral displacements) and susceptibility potential in determining the safety factor (SF) for shallow sloping and soil is assumed as isometric material properties and groundwater flow model as transient flow.

2. BASIC THEORY

2.1 Soil water characteristic curves (SWCC)

Based on the geotechnical point of view normally, aside from the previous studies, some principles or theories, including the complicated apparatus or unsaturated soil mechanics devices laboratory works, are necessary to evaluate the best-fit of soil water characteristic curves (SWCC) and to define the permeability function [15].

In unsaturated soil theory, the difference between air and hydrostatic water pressures can represented by *($u_a - u_w$)*. In the actual conditions, air pressure has always zero at the field or can be mentioned by the continuous air voids; this suction parameter can be stated in the form of *($- u_w$)* with hydrostatic pressure, which moves to the left side of soil stress cross-section [16]. If occurred the infiltration process in the rainy season, the zone of unsaturated soil can be filled out in one part by the water and form a perched water table with little movement of hydrostatic pressure to the right side or can be represented by *($+ u_w$)* in stress cross-section which is depended on the depth zone of wetting front.

In unsaturated soil analysis, SWCC defines the relation between water content and suction [17]. The SWCC describes the behavior and soil capability in conducting infiltration and/ or groundwater storage processes, which depends on the grain size distribution model according to the soil type. The SWCC model consists of 3 (three) conditions to represent the desaturation zone in a soil type, including the boundary, transition, and residual conditions, as shown in Figure 1 [18].

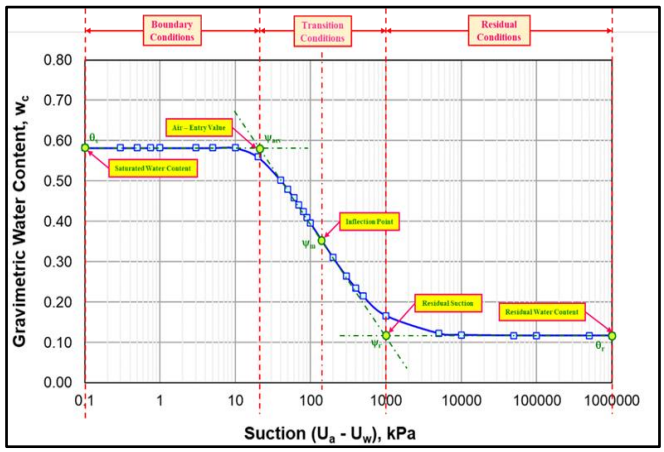

Figure 1. The phases of SWCC modeling [16]

There are some parameters to perform a best fit in modeling SWCC; among them are saturated water content *(θ_s)*, which describes the soil behavior and maximal capability to infiltrate and storage the water during the wetting process, especially during the rainy season. Suppose the air pressure has filled out partially soil pore to reach the ultimate condition with signed by the difference of a quite large pressure between air and water. In that case, this condition can be meant as the magnitude of air entry absorbed by soil pore represented as *(ψ_{aev})* [19]. When the increasing of suction occurs in a short time, which correlates to the desaturation velocity *(δ_s)*, and it is influenced by the pattern of grain size distribution on a type of soil, so that the curve tends to decrease drastically and has the certain gradient at the middle of the curve, it can be defined as the inflection point *(ψ_m)*. Unfortunately, the distribution of data recorded in the actual measurement of the permeability coefficient at the laboratory work has some errors represented by a geometric standard deviation *(σ)* modeling process of SWCC in determining the best-fit condition. However, it can be predicted by using the equation proposed in the previous research in determining the coefficient of permeability [20]. When the increasing of suction further occurred, which has failed to perform in removing many water molecules at the soil layers, it can be represented by residual point *(ψ_r)*. The

minimum capability of the soil to perform infiltration and storage during the drying process, especially during the dry season, can be defined as residual water content (θ_r). In processing of best fit when the curve modeling of SWCC unimodally according to 6 (six) parameters (θ_s, ψ_{aev}, ψ_m, σ, ψ_r, θ_r), it can be analyzed by using the non-linear regression as the permeability function. Analysis of validation of best-fit condition of SWCC uses Eq. (1) for water content (w_c) in unsaturated conditions compared with laboratory investigation results [21, 22].

$$w_c = \left(1 - \frac{\ln\left(1+\frac{\psi}{\psi_r}\right)}{\ln\left(1+\frac{10^6}{\psi_r}\right)}\right) \cdot \left[\theta_r + \left\{(\theta_s - \theta_r) \cdot \left(1 - (\beta)\mathrm{erfc}\left(\frac{\ln\left(\frac{\psi_{aev}-\psi}{\psi_{aev}-\psi_m}\right)}{\sigma}\right)\right)\right\}\right] \quad (1)$$

2.2 Estimation of permeability function

In the soil mechanics of unsaturated soil, the coefficient of permeability is almost constant for saturated soil (k_{sat}); however, for unsaturated soil, the coefficient of permeability (k_{unsat}) is a function of the water content (w_c) [23-26]. The permeability function describes the soil behavior and soil capability in conducting water flow in the soil layer, and it depends on grain size distribution according to soil type [27]. The estimation of the permeability function is based on 3 (three) parameters (θ_s, ψ_{aev}, θ_r) in the best-fit result in defining the SWCC [28]. Normally, these best-fit of SWCC equations are mathematically continuous and governed by a few fitting parameters. The study uses normalized water content to predict permeability function (k_w) to obtain the SWCC using Eq. (2).

$$k_w = k_{sat} \cdot \frac{\int_{\ln(\psi)}^{\ln(\psi_r)} \frac{\theta_s(e^y) - \theta_s(\psi)}{e^y}\, \theta_s'(e^y) \cdot dy}{\int_{\ln(\psi_{aev})}^{\ln(\psi_r)} \frac{\theta_s(e^y) - \theta_s(\psi_{aev})}{e^y}\, \theta_s'(e^y) \cdot dy} \quad (2)$$

3. METHODS

3.1 Research implementation flowchart

Soil–water characteristic curve (SWCC) term based on permeability function can be used and is more suitable in handling unsaturated problem solutions, especially in alternating the shear strength (c ; ϕ) parameters during the wetting and drying process [29, 30]. Furthermore, recently advanced analysis of SWCC has more developed; Ng and Pang [31, 32] proposed the concept of a stress-dependent soil–water characteristic curve (SDSWCC), which is exclusively used for a state-dependent soil–water characteristic curves incorporating with the effects of two independent stress state variables (i.e., suction and net mean stress) and volume changes. Similar to SWCC, the limit equilibrium methods are most preferable for practical applications due to their long history and simplicity [33].

As the research purposes, stability analysis for the existing slope does not only use the parameters of laboratory and field test results as the primary soil data, but it also involves the parameters obtained by the best fit of the soil water characteristic curve (SWCC) and the soil permeability function. Figure 2 shows the flowchart of the research method for the stability behavior of expansive residual soil during the wetting and drying process in determining the magnitude of deformation and safety factor (SF) at the Cisadane watershed area.

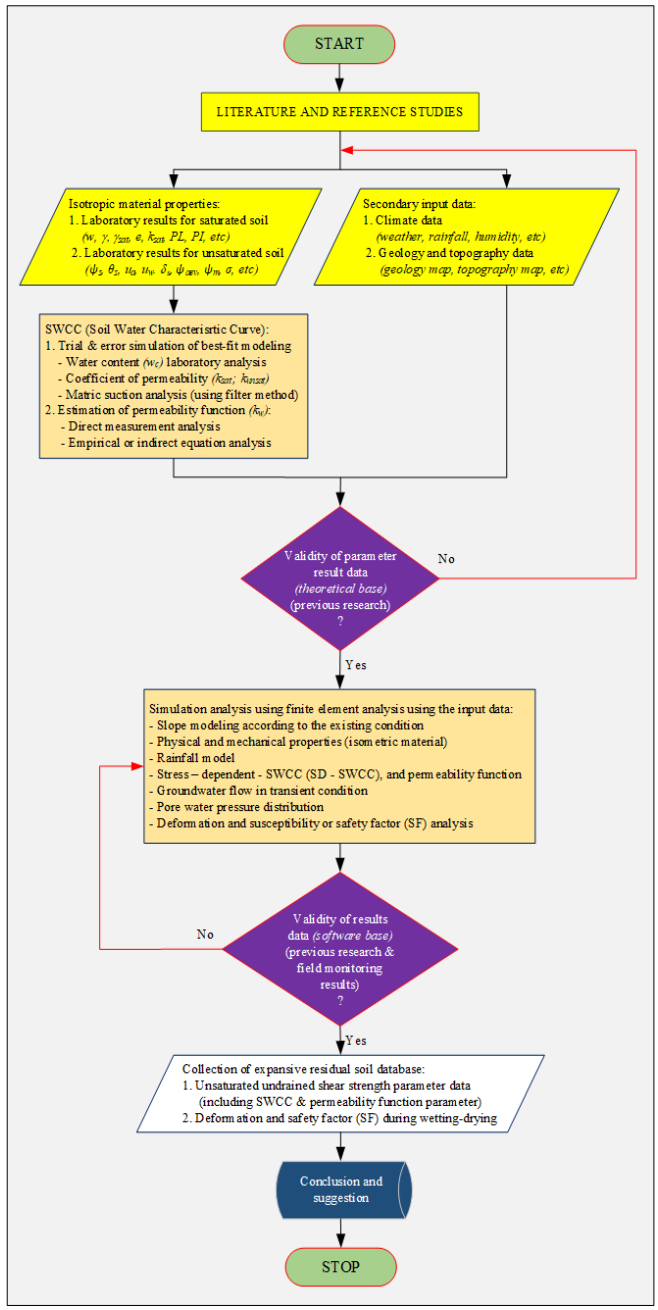

Figure 2. Flowchart implementation research

3.2 Study location

Generally, the environmental study area is South Tangerang City District, Banten Province, West Java, which has a low terrain with soft and a low hilly area. These areas exist at the elevation ± 26 – 50 meters above sea level at the northern part of the Java Sea with a slope gradient of less than 7%. Figure 3 shows the area near JLS road of Kranggan, Setu Sub-District, with the coordinate points (6° 20' 50.81"; 106° 39' 10.83"). The study location is the watershed or basin area of the Cisadane River. It can be assumed that the river flow will influence the depth of groundwater table condition and the vadose zone or unsaturated zone; finally, it will impact slope stability.

Figure 3. Sampling location of disturbed & undisturbed

3.3 Expansive residual soil sample

Disturbed and undisturbed of expansive residual samples were taken at a depth of 1.5 to 3.5 m below the ground surface. The sample-taking procedure was performed using ASTM D 1452 [34]. Then, all samples were investigated at the privately certified company for soil mechanics laboratory in East Bekasi for a detailed investigation of physical and mechanical properties. The existing condition of the disturbed sample during the sampling process performed at the study location is shown in Figure 4.

Figure 4. The typical existing condition of slope at the Cisadane watershed and / or river basin and fine-grained soil collapse during the rainy season every year

3.4 Physical and mechanical investigation

The investigation of physical and mechanical properties in determining the expansive behavior was conducted in undisturbed conditions (UDS) obtained by several points in the study area. Classification soil used the USCS (*Unified Soil Classification System*) method ASTM D2487-17e1 [35]. Furthermore, all investigations for physical and mechanical properties methods used the ASTM standard. The results of physical and mechanical properties indicated that the soil layer could be classified as a high plasticity of clay with unlimited grain size distribution patterns. Physical properties are important, as is the plasticity index (PI) value used to classify expansive soil [36]. The soil water characteristic curve (SWCC) and coefficient permeability function of soil are important input data in evaluating the deformation and landslide stability [37-39]. The application of matric suction on SWCC and water permeability function will increase accuracy in determining the safety factor (SF) values in stability analysis, which is very dependent on changes in groundwater level when compared without matric suction.

Therefore, this study is conducted to elaborate on the magnitude of deformation and stability conditions at the slope area with the ground of expansive residual layers during wetting and drying conditions. In the simulation, in determining deformation and safety factor (SF) for stability conditions by using the numerical finite element analysis of computer software, all the parameters use physical and/ or mechanical properties, which is the best fit of soil water characteristics. This study is supported by soil mechanic laboratory macro test in SWCC and permeability function analysis.

4. RESULTS AND DISCUSSION

4.1 Environmental and topography condition

The area of South Tangerang City is 147.19 km^2. The study location is very close to Jakarta, around 26 km. The study area is a low terrain with soft and low hilly areas. These areas exist at the elevation ± 26 – 50 meters above sea level at the northern part of the Java Sea with a slope gradient of less than 7%. The area has an average air temperature of around 26.4°C-28.2°C, and average air humidity is 98%. The highest rainfall is 526.8 mm, while the average rainfall is 225.9 mm every year. The highest rainfall normally occurs in January, with a duration of 25 days. The average wind speed in a year is 4.0 m/sec. Ocean areas can contribute significantly to the tropical water's condition and play an important role in the formation of alluvium deposits, especially when expansive residual soil is unsaturated, followed by negative pore-water pressures. These layers are often found in the study location, such as the Cisadane River deposit.

4.2 Geological condition

The geological conditions in this area include alluvium-diluvium deposits, tuffaceous siltstone, sandstone, and argillaceous material [40]. From a geotechnical point of view explained that the weathered process from the rock layer could result in a residual fine-grained soil layer, such as silty clay, clayey silt, sandy silt until 20 m depth, and silty sand that formed the ground surface to a depth larger than 20.0 to 30.0 m. Generally, the residual fine-grained soil originates from the weathering process of granite and/ or sedimentary rocks; the texture of residual soil depends on environmental conditions along the Cisadane River, such as the alluvium deposits at the beginning of formation. Characteristics of swelling-shrinkage are that the expansive soil is more produced by the weathering

process of basalt rock. Basalt rock can produce the montmorillonite fraction in soil.

Every year during the rainy season, the alluvium-diluvium deposit sedimented by the flow of the Cisadane River is very susceptible to the transformation of water content. The deposits can be classified as fine-grained soil classified as very to medium class of landslide susceptibility, and this vadose zone can be categorized as a shallow landslide potential reported by the local office of Vulcanology & Mitigation of Geology Disaster Center (PVMBG-Tangerang City). The swelling potential of expansive residual soils significantly depends upon wetting and shrinkage. Montmorillonite content shown by the plasticity index (PI) also plays an important role in determining SWCC and permeability function parameters. Instability or failure of expansive residual soil is primarily due to water infiltration due to high rainfall at the Cisadane watershed during the wet or rainy season. Furthermore, it is very difficult significantly to define some points in the transition phase in describing the best-fit SWCC as well, especially in determining air-entry value, inflection, and residual section point.

4.3 Physical and mechanical properties data

The standard procedure for laboratory and field soil investigation used D1586/D1586M − 18 [41] and SNI 8460 (2017) [42]. Figure 5 shows the resulting test conducted at the study area consisting of Standard Penetration Test (SPT)-borehole (BH) or boring log for sampling and Cone Penetration Test (CPT). 5 (five) BH points were performed with 6 (six) position of CPT nearly location with borlog-SPT area.

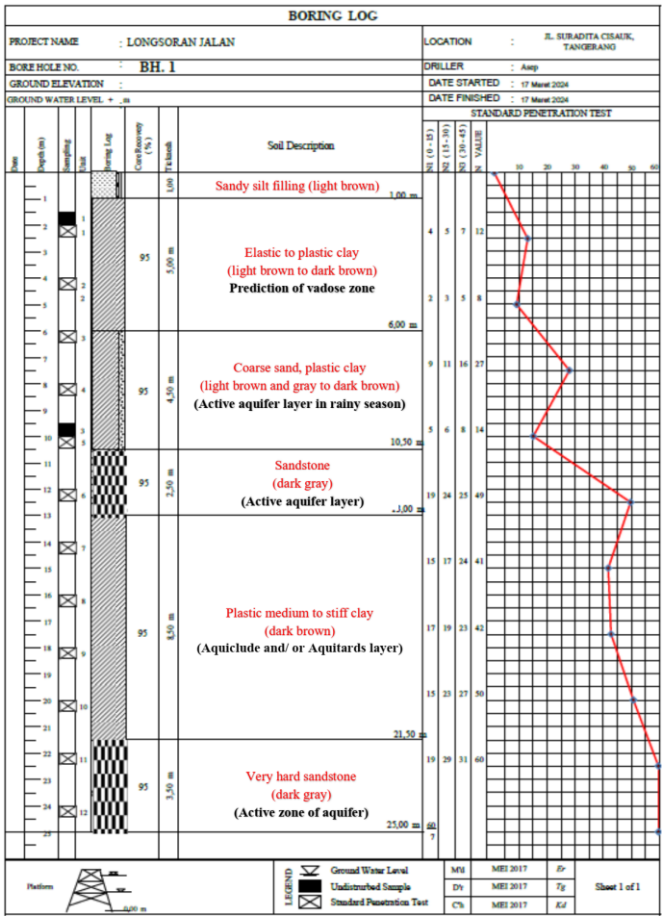

(a) Typical results of borlog-SPT

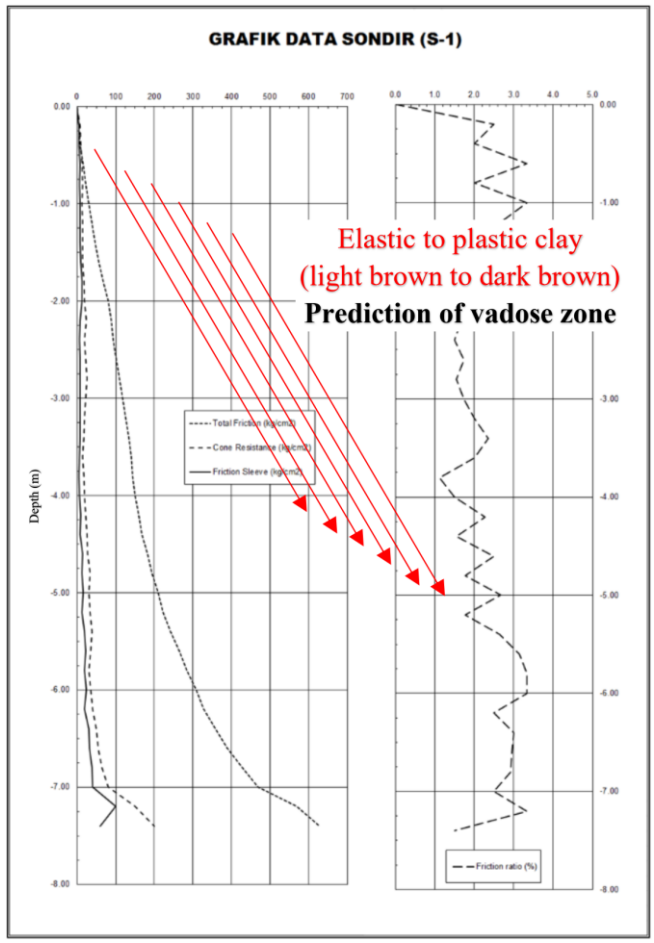

(b) Typical results of CPT

Figure 5. Typical of field test results (SPT and CPT)

Figure 5 (a) shows the typical soil layers from the SPT-BH investigation where topsoil constitutes soft sandy silt layers in brown colour from the ground surface to 1.0 m depth. At a depth of 1.0 to 6.0 m, it shows the brown elastic to plastic soft to medium stiff sandy and/ or silty clay, then it continued the medium stiff to very stiff plastic clay at a depth of 6.0 to 10.50 m. The next layer indicates hard sandstone and very stiff plastic clay, intermittently until 30.0 m depth. The interpretation of soil layers from CPT, as shown in Figure 5 (b), is determined by the graphical correlation proposed by the Robertson method [43], and the results are not so far from the results of the SPT-BH and herein the CPT test considered had failed to penetrate deeper and cannot be continued (b). The vadose zone exists from the ground surface to 5.0 or 6.0 m depth and has the number of blow (N) from 12 and 14 and cone resistance (q_c) from 0.4 to 7.0 MPa.

Table 1 shows the summary of standard laboratory work results using the macro investigation. The soil sample classification is an anorganic clay with high plasticity (CH) or A-7-5 from the ground surface to a depth of -5.00 m. It is assumed to be an unsaturated or vadose zone. In the existing condition, the river water level influences the groundwater table's fluctuation. Furthermore, PI > 30% can be assumed to be an expansive soil and create additional problems at the sensitive zone for shallow slope stability.

Table 1. Summary of physical and mechanical properties at prediction of vadose zone (-5.0 m depth from ground surface)

Physical Properties	Value Range
Liquid limit % *(LL)*	68.4 – 70.2
Plastic limit % *(PL)*	32.6 – 33.6
Plasticity index % *(PI)*	35.8 – 36.6
Liquidity index *(LI)*	0.221 – 0,467
Specific gravity *(G_s)*	2.648 – 2.650
Water content *(w_c)*	40.5 – 50.7
Gravel (%)	0.01 – 0.2
Sand (%)	2.3 – 4.1
Silt (%)	23.6 – 28.4
Clay (%)	74.0 – 67.3
Soil classification (USCS & AASHTO)	CH / A-7-5
Wet unit weight (kN/m^3)	17.22 – 18.6
Dry unit weight (kN/m^3)	12.27 – 13.45
Degree of saturation (%)	64.7 – 66.3
Mechanical Properties	**Value Range**
Cohesion *(c)*	0.21 – 0.33
Internal shear angle *(°)*	15.4 – 21.3
Saturated permeability test (m/sec)	$1.26.10^{-10}$ –$3.36.10^{-10}$

4.4 Estimation of SWCC curve

SWCC curve is the mechanical behavior of expansive residual soil represented by soil suction measurements; this study used the filter paper method. The method was selected as a conventional method of soil matric suction measurement since this method was simple for laboratory work [44]. It has been conducted the plotting for the SWCC curve unimodally during modeling simulation repeatedly based on data processing of water content *(w_c)* and soil suction *(ψ_s)*, as shown in Figure 6. Simulation of the best-fit condition was started with the appropriate initial values, including the 6 (six) parameters *(θ_s, ψ_{aev}, ψ_m, σ, ψ_r, θ_r)*. Figure 6 also indicates that the water content *(w_c)* is very influenced by temperature and humidity factors in the existing environment. This figure shows clearly that the matrix suction had the magnitude of immediately increasing during the transition condition, which was correlated with the velocity of the desaturation process *(δ_s)*. Then, this point could be an inflection point of suction *(ψ_m)*. The grain size distribution significantly influenced the magnitude of soil suction on expansive residual soil. A large fine-grained size would increase the soil's capability to infiltrate or store the water in the soil layers. These conditions would increase the magnitude of soil suction.

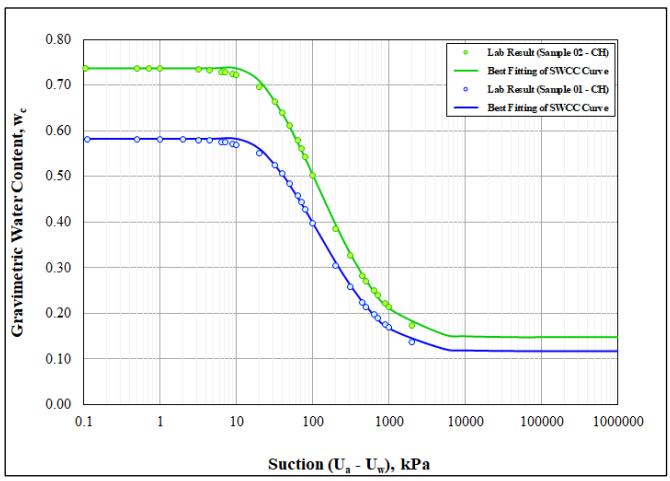

Figure 6. Plotting data results for best fit on the SWCC curve

It is possible to use the big data to determine unsaturated soil parameters in the SWCC best-fit curve model during the study; therefore, conventional probability analysis is required to determine the boundary range or condition for these parameters. Physical properties and permeability test results are very decisive in this matter. Table 2 is very helpful in plotting all values from soil suction at air-entry value, inflection, and residual section points, respectively, when the phase changes from saturated to unsaturated conditions.

Table 2. Representation values based on the SWCC best-fit curve and simplified model of laboratory saturated permeability test

Permeability Function	Range Value
k_{sat} (m/s)	$1.3.10^{-10}$ –$3.4.10^{-10}$
k_{unsat} (m/s)	3.3×10^{-14} - 8.7×10^{-13}
ψ_{aev} (kPa)	36.4 - 40.0
ψ_m (kPa)	199.5 - 200.6
ψ_r (kPa)	950 - 1,000

4.5 Estimation of permeability function

Estimating the function of permeability *(k_w)* could be conducted by simulation to determine the best fit in the SWCC curve, as shown in Figure 7. Permeability function reflected the permeability coefficient correlations between saturated *(k_{sat})* and/ or unsaturated *(k_{unsat})* conditions and soil suction *(ψ_s)*. The measurement of the coefficient of permeability was done using the laboratory falling head apparatus. The estimation of the permeability function is predicted by 3 (three) important parameters, such as θ_s, ψ_{aev}, and θ_r, in the best-fit SWCC curve simulation.

The permeability function is a determination factor in predicting every groundwater flow, and the behavior is influenced by grain distribution size. More fine-grained size would lower the capability of the soil to conduct groundwater flow and create a higher magnitude of soil suction. Table 2 shows the parameter range value of the permeability function *(k_w)* for expansive residual soil.

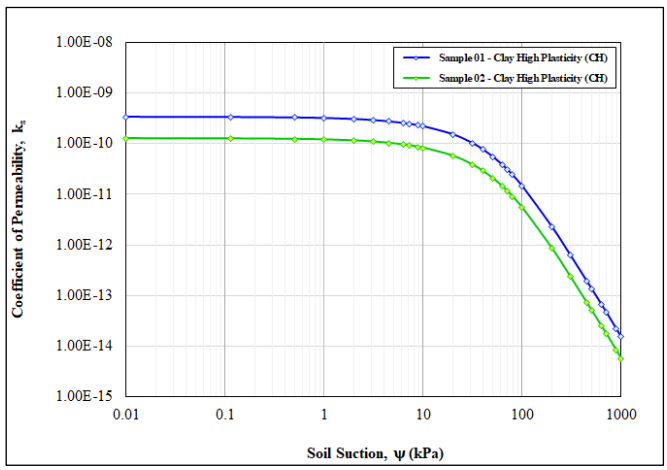

Figure 7. Permeability function and soil suction

4.6 Seepage analysis and pore water distribution

Seepage analysis forms an important and basic part of geotechnical engineering. Seepage analysis may be required in volume change prediction and fundamental changes to the wall slope. It is very difficult to determine deformation and

soil stability related to the flow model. The selection flow model of unsaturated soil plays a primary and important role, which is coupled with the change saturation-desaturation process. The saturation-desaturation process depends on microclimate and can be characterized in terms of factors such as temperature, relative humidity, wind velocity, infiltration, etc. The seepage problem, according to microclimate conditions will be related with the change of groundwater table and/or impervious boundary, respectively when the soil is saturated. However, in the case of unsaturated soil, the pore water pressure is negative in response to the imposed microclimate condition at the ground surface.

In the last two decades, the development and application of the computer to solving complex problems has been extensive. An unsaturated soil problem involves highly non-linear soil properties, such as coefficient of permeability and water storage functions. Manual analysis can be difficult because the partial differential equations to be solved are highly non-linear. This has given rise to the use of general partial differential equation solvers that are designed to solve equations from many areas of soil mechanic engineering. The solution of transient, unsaturated soil systems requires two non-linear soil property functions; the coefficient of permeability function and the water storage function. Both soil property relationships regarding the negative pore-water pressure or soil suction can be written.

Conventional analysis for groundwater flow through saturated and unsaturated soils is governed by Darcy's law. However, two major differences exist between the water flows in saturated and unsaturated soils. First, the ability of the unsaturated soils to retain water varies with soil suction. Second, the water permeability coefficient is not a constant in unsaturated soils but a function of soil suction. Thus, it is essential to define all parameters from the soil-water characteristic curve (SWCC) as shown in Figure 8 before starting seepage analysis in unsaturated soil. The seepage analysis will define the relationship between the soil suction and either the water content or the degree of saturation. The water permeability function varies with soil suction for simulating transient seepage in unsaturated soil slopes. Currently, permeability function for seepage analysis is obtained from a measured saturated and unsaturated water permeabilities in wet and drying conditions, respectively of the existing SWCC as shown in Figure 9.

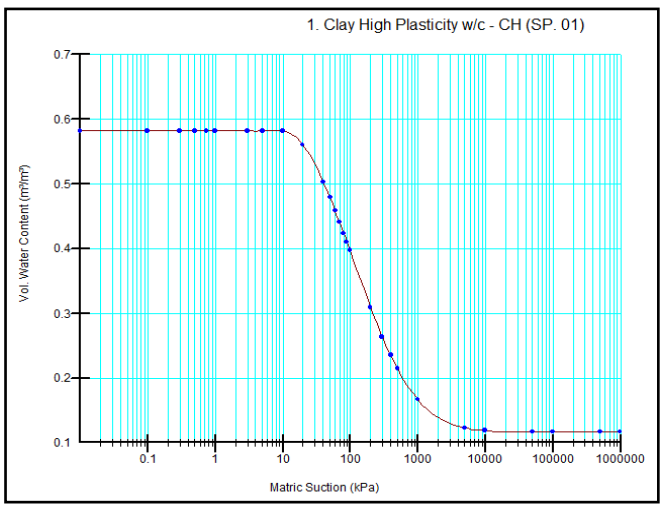

Figure 8. Parameter SWCC curve *(w_c, θ_s, k_w, and ψ_s)* on seepage analysis

Hereinafter, simulation using was conducted to model the seepage phenomenon and pore water distribution based on the laboratory measurement for water content *(w_c)*, saturated water content *(θ_s)*, permeability function *(k_w)*, and soil suction *(ψ_s)* from the approximation of SWCC the best-fit curve and permeability function parameters from Figures 8 and 9, respectively. The simulation purpose was to define the seepage model and the distribution of pore water pressure according to time magnitude, especially in the overview of every depth from the top of the slope due to the infiltration process during with and without the precipitation in dry and/ or rainy seasons.

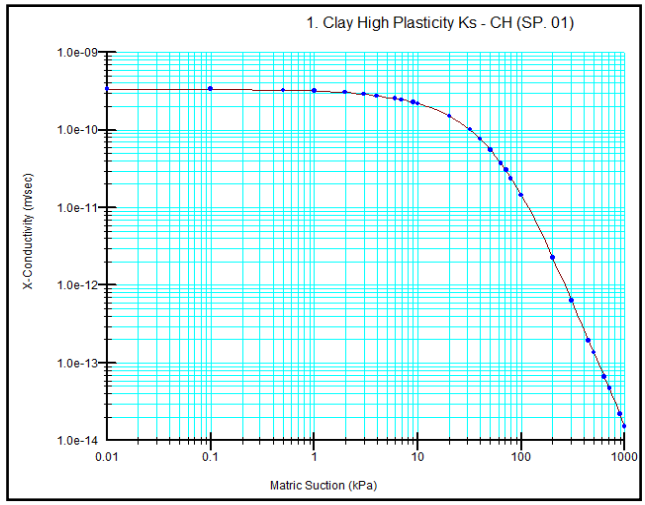

Figure 9. Permeability function in seepage analysis

Figures 8 and 9 show the existing SWCC curve after data plotting on the finite element analysis using the Seep/W, so that the analytical approach results from Figures 6 and 7 must be matched with Figures 8 and 9, respectively each other before they are used as input data on seepage analysis and pore water distribution. Figure 8 and 9 also indicates that the parameter of permeability function *(k_w)*, soil suction *(ψ_s)*, and saturated coefficient permeability *(k_{sat})* from estimation of permeability function as the input data were used in analyzing of seepage phenomenon in steady state and transient on expansive residual soil. The seepage analysis in transient conditions was observed during the maximum intensity of rainfall or precipitation data in the rainy season in the study area [45, 46].

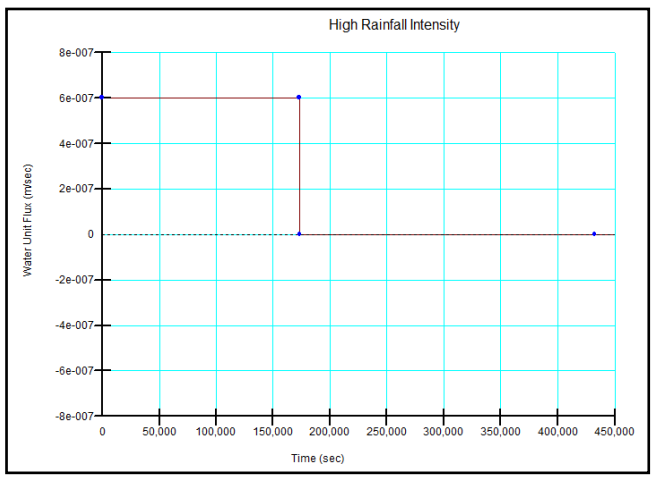

Figure 10. Intensity of maximum rainfall model as the input data on finite element simulation during seepage analysis

The rainfall data were obtained from Meteorological, Climatological, and Geophysics (BMKG-Tangerang City). Research on the pattern and intensity of rainfall in the city of Rainfall data consists of the pattern and intensity of rainfall. This study conducted pattern analysis and intensity of rainfall in the years 2020 to 2025; there is one data used in this analysis, including the rain observation data at station officials, which is close to the study area.

Figure 10 shows that the seepage analysis was conducted with a groundwater depth of (–) 1.20 m at the study location around Jalan. JLS (Jalan Lingkar Selatan) and (–) 1.50 m at near of Cisadane River. Rainfall intensity in the Tangerang District area was around 13.528 mm/day or 1.566 x 10^{-7} m/s. During the wetting condition, seepage analysis was calculated for 2 (two) days from the first rainy day, and during the drying condition, it was reviewed 3 (three) on the next day.

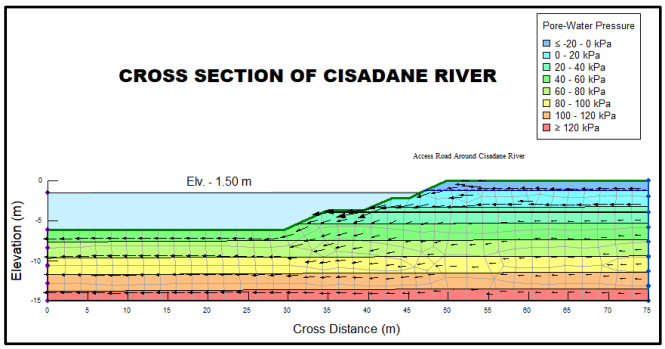

(a) Contour modeling of pore water pressure (PWP) for t = 0.00 days

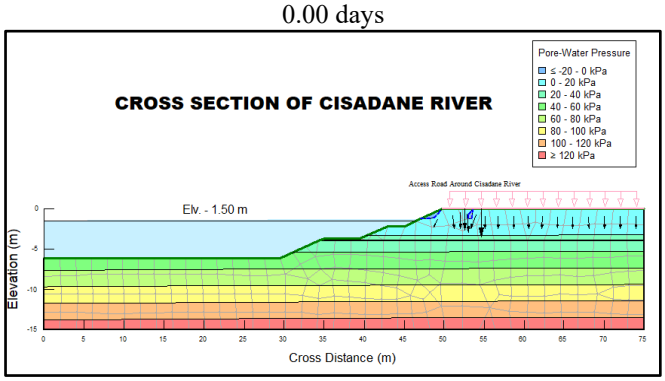

(b) Contour modeling of pore water pressure (PWP) for t = 0.13 days

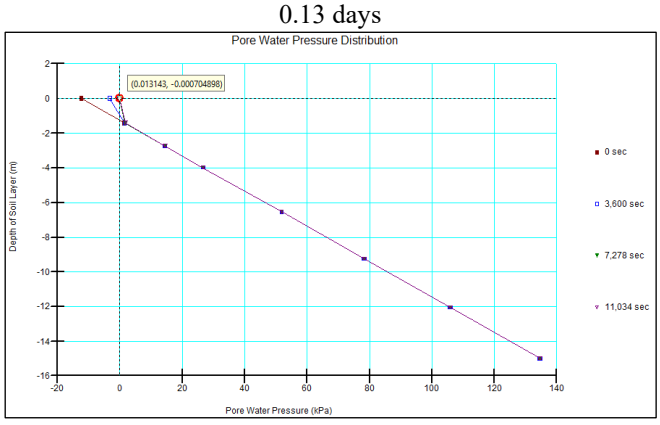

(c) Pore water pressure distribution (PWP) during t = 0.00 to 0.13 days

Figure 11. Modeling of contour and pore water pressure (PWP) distribution (t = 0.00 to 0.13 days) *(Seep/W analysis)*

Figure 11 shows that the rainwater precipitation performed a desaturation process to the unsaturated soil layer during 0.00 to 0.13 days (11,034 seconds or 3.07 hours) through the gap and/ or soil pore. Negative pore water pressure was also conducted in closing to equilibrium hydrostatic line condition with the tension from (–) 0.00070 kPa to (–) 12.403 kPa.

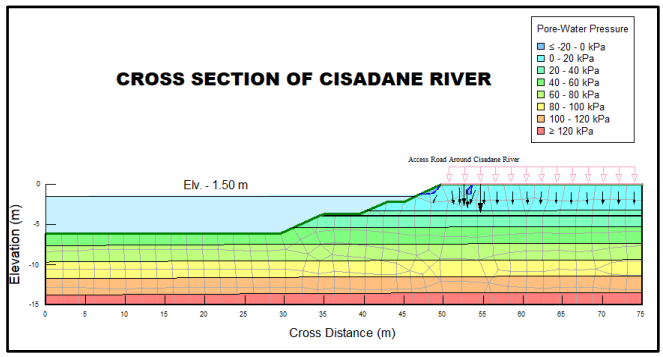

(a) Contour modeling of pore water pressure (PWP) for 0.13 days

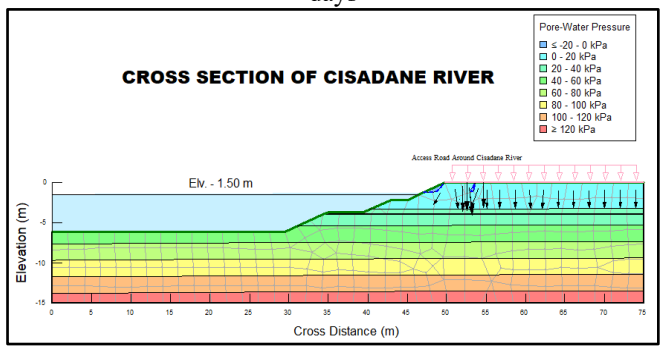

(b) Contour modeling of pore water pressure (PWP) for t = 0.17 days

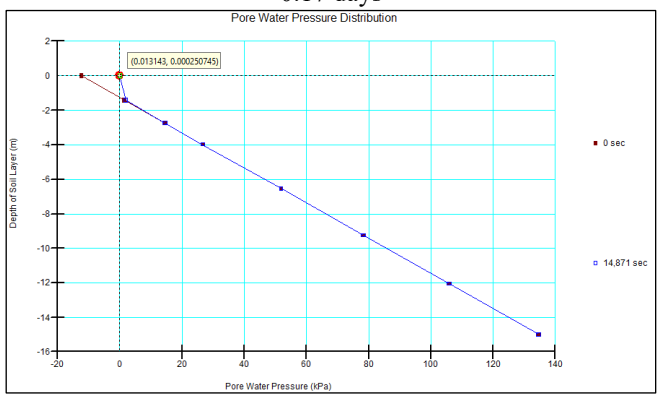

(c) Pore water pressure distribution (PWP) during t = 0.13 to 0.17 days

Figure 12. Pore water pressure distribution (PWP) during (t = 0.13 to 0.17 days) *(Seep/W analysis)*

Figure 12 indicates that the water rainfall was successful in the desaturation process of all ground surfaces at the unsaturated zone for 0.17 days (14,871 seconds or 4.13 hours), and tension of cross-section had reached the equilibrium hydrostatic condition with negative pore water pressure of (+) 0.00025 kPa in the stress cross-section.

In this study, practical applications of unsaturated soil mechanics are time-consuming and expensive unsaturated soil laboratory tests in determining engineering properties. The accuracy of the prediction of the SWCC best-fit curve and permeability function really produces a good result and is validated by shallow slope conditions in the field. Figure 12 is the first simulation analysis due to infiltration during rainfall here; three predictions can be drawn from this work such as

high-intensity rainfall can rapidly transform soil surface features of shallow bare soil; in the vadose zone, shallow slopes are more easily eroded than nearby steep slopes, and there is a more pronounced lowering of the ground surface due to compaction and denser microlayers on gentler slopes.

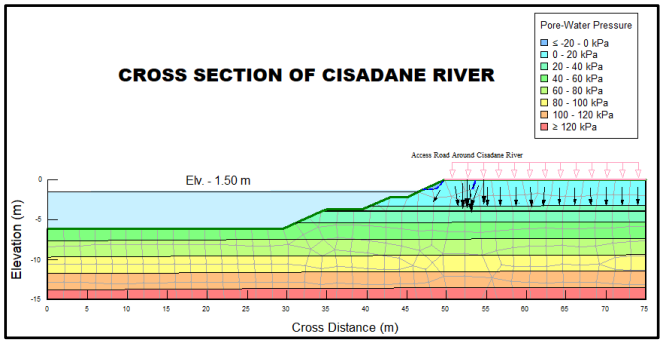

(a) Contour modeling of pore water pressure (PWP) for 0.22 days

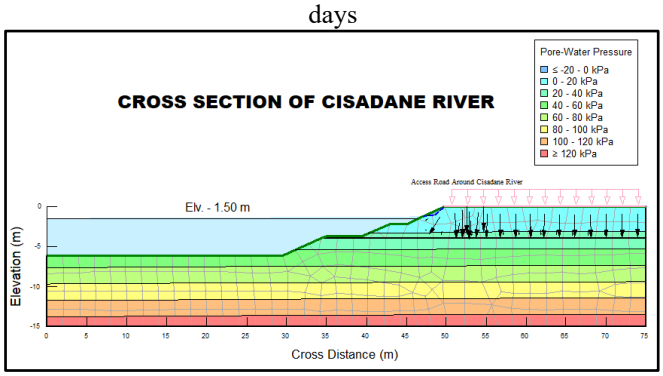

(b) Contour modeling of pore water pressure (PWP) for 1.97 days

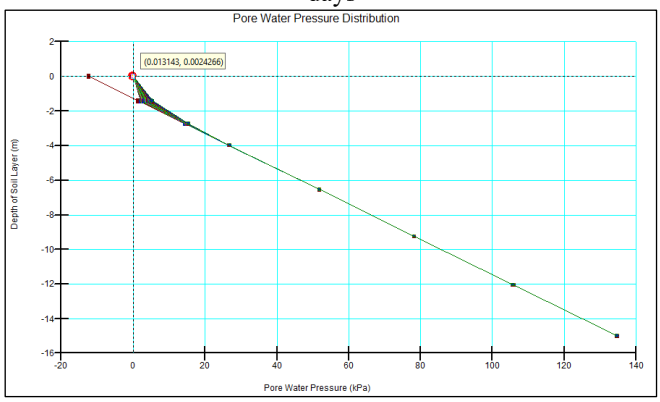

(c) Pore water pressure distribution (PWP) during 0.22 to 1.97 days

Figure 13. Pore water pressure distribution (PWP) during t = 0.22 to 1.97 days *(Seep/W analysis)*

Figure 13 shows that the water rainfall has already finished the desaturating process from all pores at saturated soil layers for 0.22 days (18,790 seconds or 5.22 hours) to 1.97 days (170,299 seconds or 47.31 hours). Infiltration capacity and water storage at the ground layers are already in perfect saturation condition. Finally, the water rainfall could overflow to the low level of the Cisadane River, with each negative pore water pressure of (+) 0.00037 kPa and (+ 0.00243 kPa), respectively.

Figure 14 indicates that at the time of 2.06 days (177,554 seconds or 49.32 hours) to 5.00 days (432,000 seconds / 120.00 hours). The negative pore water pressure has been trying to move away from the equilibrium hydrostatic line of the cross-section or move back towards the initial hydrostatic condition because the rainfall has been stopped, and occurred the water rainfall during the evaporation process in unsaturated soil layers, finally negative pore water pressure increased significantly with each of (–) 0.330 kPa and (–) 5.968 kPa in stress cross section.

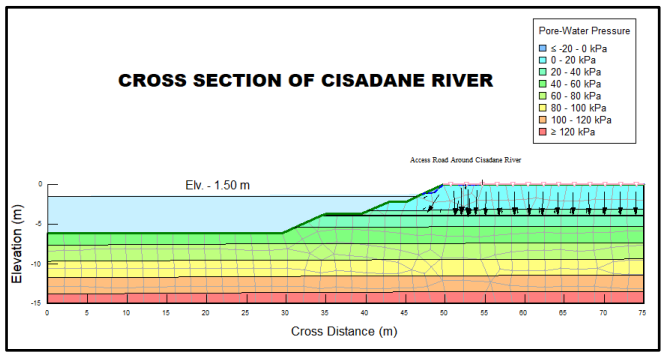

(a) Contour modeling of pore water pressure (PWP) for 2.06 days

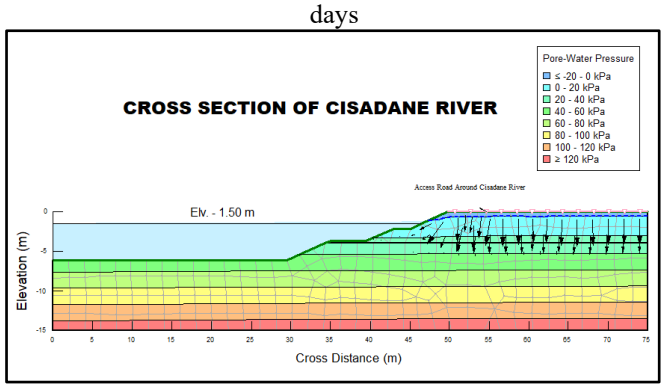

(b) Contour modeling of pore water pressure (PWP) for 5.00 days

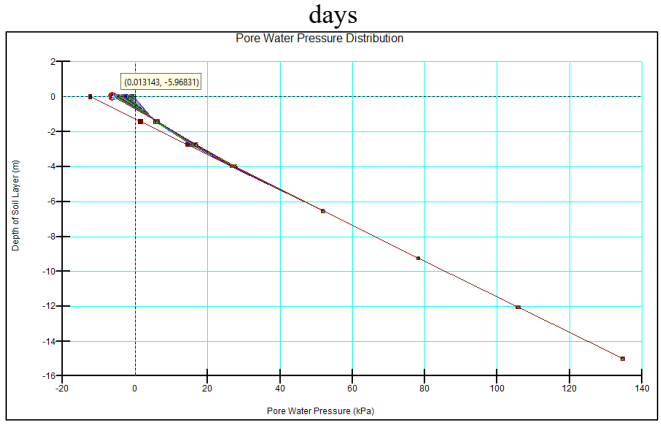

(c) Pore water pressure distribution (PWP) during 2.06 to 5.00 days

Figure 14. Pore water pressure distribution (PWP) during t = 2.06 to 5.00 days *(Seep/W analysis)*

Based on Figure 14, it can be concluded that a decrease in the swelling ability of unsaturated expansive clays corresponds to a reduced water absorption capability when the soils were alternately wetted and partially shrunk. On the other hand, an increase in the swelling potential was noted when the soils were fully shrunk. In either case, equilibrium can be attained after several cycles. As the number of cycles increases, further destruction of large and disorientation of particle structure.

4.7 Slope stability and deformation analysis

Slope stability and deformation analysis were conducted using finite element analysis using the Geostudio software program. This modeling aims to determine the magnitude of stability (safety factor) and deformation on slopes analyses of expansive residual soil due to wetting and drying conditions. The simulation slope stability and deformation results are shown in Figure 15. The soil water characteristic curve (SWCC) as the best-fit curve should be selected to investigate the hydraulic properties of unsaturated soil because it is closely related to the matric suction and the water content of the unsaturated soil. The best-fit curve representing the volumetric water content verse matric suction results from the hydraulic parameter of SWCC before landslides occurred. From Figure 15, it would be indicated that the positive pore water pressure changes gradually increase during the rainy season and vice versa to negative during the dry season.

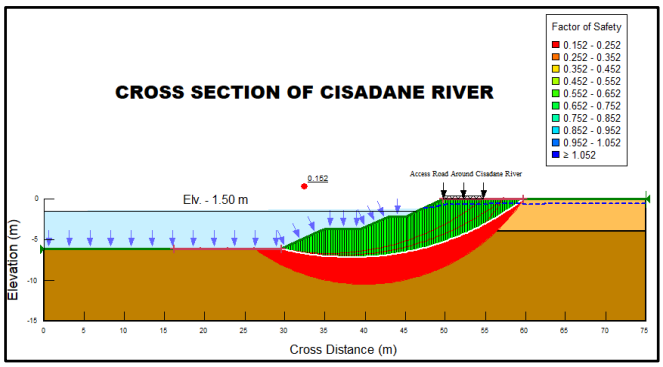

(a) Simulation stability model during the rainy season

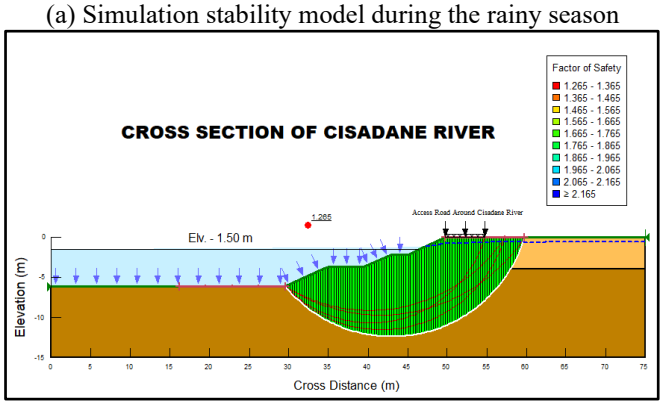

(b) Simulation stability model during the dry season

Figure 15. Analysis results of stability analysis during rainy and dry seasons *(Slope/W analysis)*

Figure 15 (a) also shows that the results of finite element simulations indicate that the critical safety factor (SF) during the wetting condition where the infiltration process occurred in the rainy season obtained SF = 0.152. Drying conditions or evaporation processes, as shown in Figure 15 (b), that occurred during the dry season resulted in SF = 1.265. The magnitude of deformation could be obtained at 4.304 cm or 43.040 mm (according to the y-axis direction) and 3.836 cm or 38.360 mm (according to the x-axis direction) during wetting conditions or infiltration process. During dry conditions or evaporation, it could indicate 0.471 cm or 4.710 mm and 0.214 cm atau 2.141 mm according to y and x-axis directions, respectively.

The magnitude of deformation could be obtained at 4.304 cm or 43.040 mm (according to the y-axis direction) and 3.836 cm or 38.360 mm (according to the x-axis direction) during wetting conditions or infiltration process. During dry conditions or evaporation, it could indicate 0.471 cm or 4.710 mm and 0.214 cm or 2.141 mm according to y and x-axis directions, respectively.

Soil behavior and the properties of unsaturated residual soils can have swelling potential and shrinkage potential. In the area study, these layers exist from the ground surface to a depth of -5.00 m. Based on the theory and practice of unsaturated soils, several efforts must be made to maintain the water content (w_c) under infrastructure construction through the simulation of slope stability and deformation analysis of the road. The topographic conditions located next to the river mean several drainage control factors must be considered, including the drainage system, settlement, groundwater infiltration, erosion by river flows, and upward pressure (up-lift). An integrated analysis should be elaborated through rainfall, laboratory and field tests, and numerical analysis.

The research study's purpose was to determine the magnitude of deformation and stability conditions at soil slopes due to wetting and drying conditions, and curve (SWCC) was considered during the simulation. The simulation results indicated that the dry season was more stable than the rainy season. Deformation during dry conditions was smaller than 1.0 inch (25,4 mm), with the safety value (SF) of slope sliding larger than 1.20. The opposite would occur during wet conditions or the rainy season.

Assessment and analysis of SWCC and the selection of permeability function were very crucial in stability analysis on unsaturated expansive residual soil [47]. Existing conditions and field observation must be considered carefully to validate the simulation results. Rigorous laboratory analysis, especially during the measurement of the moisture water content (w_c), saturated water content (θ_s), permeability function (k_w) and soil suction (ψ_s), and the estimation for unsaturated and saturated permeability $(k_{unsat};\ k_{sat})$ respectively must be performed to avoid some errors in assessment SWCC and permeability function (k_w) [48]. Some errors in the determination of SWCC and permeability function (k_w) would cause some mistakes in defining the safety factor (SF).

Another point obtained from the research field observation is related with the characteristic of expansive soil, which expands when the moisture content of the soil increases. The clay mineral of montmorillonite is mainly responsible for swelling and shrinkage potential. Expansive soils are generally residual soil left in the place of their formation after the chemical decomposition of the rocks, such as Basalt found in this study area; expansive soils could be saturated and/ or unsaturated condition. These lands are generally dry because the outflow of water from springs are quite large, as can be seen on the Cisadane River dyke or embankment. During the rainy season, they become wet. The swelling – shrinkage as the water content fluctuation- normally begins from small cracks to fractures. Severe movement of the soil mass may occur. Structures built on such soils may experience cracking & damage due to differential heave or instability with the lowest safety value (SF) during the rainy season. In yearly, repairs to the damages of road body structures are always carried out in this area because they are not taken seriously in studying behavior of unsaturated expansive residual soil. The average active zone at this study area is less than 5.0 m depth, as well as the plotting the liquidity index (LI) and/ or plasticity index (PI) against depth. From observation, normally, the initial movement of unsaturated expansive soil material was occurred at the one third to the maximum depth of these layers.

It could be deduced that the swelling process was triggered by the sliding potential at the study location in heavy rainfall.

5. CONCLUSION AND SUGGESTION

The capability of expansive residual soil was simulated during rainy and dry seasons by estimation measurement of laboratory SWCC curve and permeability function. Laboratory analysis is an important factor in analyzing the seepage in transient conditions (wetting or infiltration process) and steady state (drying or evaporation process). The sensitivity layer of expansion residual soil existed at 5.0 to 10.0 m depth. The critical safety factor (SF) during wetting conditions where infiltration occurred in the rainy season obtained SF = 0.152. And, during drying or evaporation in the dry season, it resulted in SF = 1.265.

In area study, the simulation model of deformation and slope stability analysis considered the effects of rainfall, existing conditions of the environment, and physical and/ or mechanical properties. The best fit of the SWCC model, the permeability function, was defined, considering the infiltration analysis based on the precipitation potential model from the study area. The failure zone of slope as the ground effect was evaluated by the influence of matric suction to the depth of -5.00 m. The study results can emphasize that rainfall infiltration due to the precipitation model of rainfall potential event was responsible for triggering the observed landslide failure.

The results of this study have shown that the cyclic swelling process due to the wetting and drying process leads to a gradual destruction of the contacts in the unsaturated expansive soil structure. At the same time, a reconstruction and reorientation of the particle structure will create a change in the shear strength parameter $(c;\phi)$. The increasing number of swelling-shrinkage cycles and the weakening process also continue if the slope area is left without improvement efforts.

Generally, the results of the simulation process agree closely with the results of the existing site investigation. The selected research method can be appropriate for simulating the landslide potential in unsaturated residual soils. This methodology illustrated that the application in determining deformation and slope stability is consistent with defining the critical slip surfaces corresponding to the minimum factor of safety (SF) and is reasonable agreement as observation works.

ACKNOWLEDGMENT

The authors would like to thank P3M Politeknik Negeri Jakarta for funding this research through the Basic Research Grant No.: 374/PL3.A.10/PT.00.06/2024.

REFERENCES

[1] Yang, R., Xiao, P., Qi, S. (2019). Analysis of slope stability in unsaturated expansive soil: A case study. Frontiers in Earth Science, 7: 292. https://doi.org/10.3389/feart.2019.00292

[2] Sudjianto, A.T., Susilo, S.H., Tolan, P.M., Agung, P.A.M., Hasan, M.F.R. (2023). Increasing the stability of expansive soil using LAPINDO sediments materials. International Journal of GEOMATE, 25(108): 154–162. https://doi.org/10.21660/2023.108.3767

[3] Jeong, S., Lee, K., Kim, J., Kim, Y. (2017). Analysis of rainfall-induced landslide on unsaturated soil slopes. Sustainability, 9(7): 1280. https://doi.org/10.3390/su9071280

[4] Wu, L.Z., Zhu, S.R., Peng, J. (2020). Application of the Chebyshev spectral method to the simulation of groundwater flow and rainfall-induced landslides. Applied Mathematical Modelling, 80: 408–425. https://doi.org/10.1016/j.apm.2019.11.043

[5] Sorbino, G., Nicotera, M.V. (2013). Unsaturated soil mechanics in rainfall-induced flow landslides. Engineering Geology, 165: 105–132. https://doi.org/10.1016/j.enggeo.2012.10.008

[6] Kim, J., Lee, K., Jeong, S., Kim, G. (2014). GIS-based prediction method of landslide susceptibility using a rainfall infiltration-groundwater flow model. Engineering Geology, 182: 63–78. https://doi.org/10.1016/j.enggeo.2014.09.001

[7] Gui, M.W., Wu, Y.M. (2014). Failure of soil under water infiltration condition. Engineering Geology, 181: 124–141. https://doi.org/10.1016/j.enggeo.2014.07.005

[8] Chen, K., He, X., Liang, F., Sheng, D. (2024). Strength and dilatancy of an unsaturated expansive soil at high suction levels. Journal of Rock Mechanics and Geotechnical Engineering. https://doi.org/10.1016/j.jrmge.2024.05.061

[9] Huat, B.B.K., Ali, F.H., Abdullah, A. (2005). Shear strength parameters of unsaturated tropical residual soils of various weathering grades. Electronic Journal of Geotechnical Engineering, 10(6): 1–16.

[10] Chang, W.J., Chou, S.H., Huang, H.P., Chao, C.Y. (2021). Development and verification of coupled hydro-mechanical analysis for rainfall-induced shallow landslides. Engineering Geology, 293: 106337. https://doi.org/10.1016/j.enggeo.2021.106337

[11] Cascini, L., Cuomo, S., Pastor, M., Sorbino, G. (2010). Modeling of rainfall-induced shallow landslides of the flow-type. Journal of Geotechnical and Geoenvironmental Engineering, 136(1): 85–98. https://doi.org/10.1061/(ASCE)GT.1943-5606.0000182

[12] Rezaei, M., Ajalloeian, R., Ghafoori, M. (2012). Geotechnical properties of problematic soils emphasis on collapsible cases. International Journal of Geosciences, 3(1): 105–110. https://doi.org/10.4236/ijg.2012.31012

[13] Zhou, W.H., Yin, Z.Y., Yuen, K.V. (2021). Practice of Bayesian Probability Theory in Geotechnical Engineering. Singapore: Springer Singapore. https://doi.org/10.1007/978-981-15-9105-1

[14] Griffiths, D.V, Gordon, A.F. (2007). Probabilistic Methods in Geotechnical Engineering. Berlin: Springer Science & Business Media. https://doi.org/10.1007/978-3-211-73366-0

[15] Ribolzi, O., Patin, J., Bresson, L.M., Latsachack, K.O., Mouche, E., Sengtaheuanghoung, O., Silvera, N., Thiébaux, J.P., Valentin, C. (2011). Impact of slope gradient on soil surface features and infiltration on steep slopes in northern Laos. Geomorphology, 127(1–2): 53–63. https://doi.org/10.1016/j.geomorph.2010.12.004

[16] Briaud, J.L. (2023). Geotechnical Engineering: Unsaturated and Saturated Soils. New York: John Wiley & Sons.

[17] Liu, C.Y., Ku, C.Y., Huang, C.C., Lin, D.G., Yeih, W.C. (2015). Numerical solutions for groundwater flow in unsaturated layered soil with extreme physical property contrasts. International Journal of Nonlinear Sciences and Numerical Simulation, 16(7–8): 325–335. https://doi.org/10.1515/ijnsns-2015-0060
[18] Zhai, Q., Rahardjo, H., Satyanaga, A. (2019). Estimation of air permeability function from soil-water characteristic curve. Canadian Geotechnical Journal, 56(4): 505–513. https://doi.org/10.1139/cgj-2017-0579
[19] Fredlund, D.G., Rahardjo, H., Fredlund, M.D. (2012). Unsaturated soil mechanics in engineering practice. Journal of Geotechnical and Geoenvironmental Engineering, 132(3): 286–321. https://doi.org/10.1061/(ASCE)1090-0241(2006)132:3(286)
[20] Fredlund, D.G., Xing, A., Huang, S. (1994). Predicting the permeability function for unsaturated soils using the soil-water characteristic curve. Canadian Geotechnical Journal, 31(4): 533–546. https://doi.org/10.1139/t94-062
[21] Chin, K.B., Leong, E.C., Rahardjo, H. (2010). A simplified method to estimate the soil-water characteristic curve. Canadian Geotechnical Journal, 47(12): 1382–1400. https://doi.org/10.1139/T10-033
[22] He, X., Cai, G., Sheng, D. (2025). Indirect models for SWCC parameters: Reducing prediction uncertainty with machine learning. Computers and Geotechnics, 177: 106823. https://doi.org/10.1016/j.compgeo.2024.106823
[23] Zhai, Q., Rahardjo., H. (2015). Estimation of permeability function from the soil–water characteristic curve. Engineering Geology, 199: 148–156. https://doi.org/10.1016/j.enggeo.2015.11.001
[24] Li, J.L., Zhang, L.M., Li, X. (2011). Soil-water characteristic curve and permeability function for unsaturated cracked soil. Canadian Geotechnical Journal, 48(7): 1010–1031. https://doi.org/10.1139/t11-027
[25] Satyanaga, A., Rahardjo, H., Zhai, Q. (2017). Estimation of unimodal water characteristic curve for gap-graded soil. Soils and Foundations, 57(5): 789–801. https://doi.org/10.1016/j.sandf.2017.08.009
[26] Ng, C.W.W., Zhan, L.T., Bao, C.G., Fredlund, D.G., Gong, B.W. (2003). Performance of unsaturated expansive soil slope subjected to artificial rainfall infiltration. Geotechnique, 53(2): 143–157. https://doi.org/10.1680/geot.2003.53.2.143
[27] Gao, Z., Chai, J. (2022). Method for predicting unsaturated permeability using basic soil properties. Transportation Geotechnics, 34: 100754. https://doi.org/10.1016/j.trgeo.2022.100754
[28] Zhai, Q., Rahardjo, H., Satyanaga, A. (2017). Effects of residual suction and residual water content on the estimation of permeability function. Geoderma, 303: 165–177. https://doi.org/10.1016/j.geoderma.2017.05.019
[29] Tarantino, A., Tombolato, S. (2005). Coupling of hydraulic and mechanical behavior in unsaturated compacted clay. Geotechnique, 55(4): 307–317. https://doi.org/10.1680/geot.2005.55.4.307
[30] Schmidt, K.M., Roering, J.J., Stock, J.D., Dietrich, W.E., Montgomery, D.R., Schaub, A.T. (2001). The variability of root cohesion as an influence on shallow landslide susceptibility in Oregon Coast Range. Canadian Geotechnical Journal, 38(5): 995–1024. https://doi.org/10.1139/t01-031
[31] Ng, C.W.W., Pang, W.Y. (2000). Influence of stress state on soil-water characteristics and slope stability. Journal of Geotechnical and Geoenvironmental Engineering, 126(2): 157–166. https://doi.org/10.1061/(ASCE)1090-0241(2000)126:2(157)
[32] Ng, C.W.W., Menzies, B. (2007). Advanced unsaturated Soil Mechanics and Engineering. London: CRC Press. https://doi.org/10.1201/9781482266122
[33] Agung, P.A.M., Hasan, M.F.R., Susilo, A., Ahmad, M.A., Ahmad, M.J.B., Abdurrahman, U.A., Sudjianto, A.T., Suryo, E.A. (2023). Compilation of parameter control for mapping the potential landslide areas. Civil Engineering Journal, 9(4): 974–989. https://doi.org/10.28991/CEJ-2023-09-04-016
[34] ASTM D 1452. (2016). Standard Practice for Soil Exploration and Sampling by Auger Borings. United States: American Standard Testing and Material.
[35] ASTM D2487-17e1. (2020). Standard Practice for Classification of Soils for Engineering Purposes (Unified Soil Classification System). United States: American Standard Testing and Material.
[36] Basma, A.A., Al-Homoud, A.S., Malkawi, A.I.H., Al-Bashabsheh, M.A. (1996). Swelling-shrinkage behavior of natural expansive clays. Applied Clay Science, 11(2–4): 211–227. https://doi.org/10.1016/S0169-1317(96)00009-9
[37] Mualem, Y. (1976). A new model for predicting the hydraulic conductivity of unsaturated porous media. Water Resources Research, 12(3): 513–522. https://doi.org/10.1029/WR012i003p00513
[38] Genuchten, M.T.V. (1980). A closed-form equation for predicting the hydraulic conductivity of unsaturated soils. Soil Science Society of America, 44(5): 892–898. https://doi.org/10.2136/sssaj1980.03615995004400050002x
[39] Sidiropoulos, E., Yannopoulos, S. (1993). A comparative study of closed-form hydraulic conductivity prediction models. Advances in Water Resources, 16(6): 317–329. https://doi.org/10.1016/0309-1708(93)90012-5
[40] Turkandi, T., Sudarto, Agustiyanto, D.A., Hadiwidjoyo, M.M.P. (1992). Geologic map of Jakarta and Kepulauan Seribu Quadrangles, Java. Bandung: Geological Research and Development Centre.
[41] ASTM D1586/D1586M-18e1. (2022). Standard Test Method for Standard Penetration Test (SPT) and Split-Barrel Sampling of Soils. United States: American Standard Testing and Material.
[42] SNI 8460. (2017). Persyaratan perancangan geoteknik (Geotechnical design requirements). Jakarta: Badan Standardisasi Nasional.
[43] Robertson, P.K. (2011). Interpretation of cone penetration test-A unified approach. Canadian Geotechnical Journal, 46(11): 1337–1355. https://doi.org/10.1139/T09-065
[44] Bulut, R., Lytton, R.L., Wray, W.K. (2001). Soil suction measurements by filter paper. Expansive Clay Soils and Vegetative Influence on Shallow Foundations, 243–261. https://doi.org/10.1061/40592(270)14
[45] Chen, C.C., Chen, T.C., Yu, F.C., Lin, S.C. (2005). Analysis of time-varying rainfall infiltration induced landslide. Environmental Geology, 48: 466–479. https://doi.org/10.1007/s00254-005-1289-z
[46] Indrawan, I.G.B., Rahardjo, H., Leong, E.C. (2007). Drying and wetting characteristics of a two-layer soil

column. Canadian Geotechnical Journal, 44(1): 20–32. https://doi.org/10.1139/t06-090
[47] Nowamooz, H., Jahangir, E., Masrouri, F. (2013). Volume change behaviour of a swelling soil compacted at different initial states. Engineering Geology, 153(3): 25–34. https://doi.org/10.1016/j.enggeo.2012.11.010
[48] Zhang, J., Tong, J., Wang, X., Liu, C., Huang, Z. (2018). Influences of drying and wetting cycles and compaction degree on strength of yudong silt for subgrade and its prediction. Advances in Civil Engineering, 2018: 1364186. https://doi.org/10.1155/2018/1364186

NOMENCLATURE

CPT	Cone penetration test
DS	Disturbed sample
GIS	Geographic information system
PWP	Pore water pressure distribution
SWCC	Soil water characteristic curve
LL	Liquid limit
PL	Plastic limit
PI	Plasticity index
SPT	Standard penetration test
UDS	Undistubed sample
LI	Liquidity index
SF	Safety factor
USCS	Unified soil classification system
AASHTO	American Association of State Highway and Transportation Officials
YS-model	YonSei-Slope model analysis

Greek symbols

(c)	Cohesion parameter
(δ_s)	Desaturation velocity
(ϕ)	Internal shear strength
(fs)	friction sleeve of CPT
(F_R)	Friction ratio of CPT
(k_w)	Permeability function
(k_{unsat})	Unsaturated permeability
(k_{sat})	Saturated permeability
(N)	Number of blow (SPT)
(S_r)	Degree of saturation
(t)	Time
(σ)	Geometric deviation standard
(q_c)	Cone resistance of CPT
(u_a)	Air pressure
(θ_s)	Volumetric saturated water content
(θ_r)	Volumetric residual water content
($u_a - u_w$)	Matric suction
($- u_w$)	Negative pore water pressure
($+ u_w$)	Positive pore water pressure
(w_c)	Moisture water content
(ψ_{aev})	Soil suction at air-entry value
(ψ_r)	Soil suction at residual section
(ψ_s)	Soil suction
(ψ_m)	Soil suction at inflection point